

Fission Yeast Cut8 Is Required for the Repair of DNA Double-Strand Breaks, Ribosomal DNA Maintenance, and Cell Survival in the Absence of Rqh1 Helicase[∇]

Stephen E. Kearsey,¹ Abigail L. Stevenson,¹ Takashi Toda,² and Shao-Win Wang^{1*}

Department of Zoology, University of Oxford, South Parks Road, Oxford OX1 3PS, United Kingdom,¹ and Cell Regulation Laboratory, London Research Institute, Cancer Research UK, 44 Lincoln's Inn Fields, London WC2A 3PX, United Kingdom²

Received 11 August 2006/Returned for modification 19 September 2006/Accepted 6 December 2006

***Schizosaccharomyces pombe* Rqh1 is a member of the RecQ DNA helicase family. Members of this protein family are mutated in cancer predisposition diseases, causing Bloom's, Werner, and Rothmund-Thomson syndromes. Rqh1 forms a complex with topoisomerase III and is proposed to process or disrupt aberrant recombination structures that arise during S phase to allow proper chromosome segregation during mitosis. Intriguingly, in the absence of Rqh1, processing of these structures appears to be dependent on Rad3 (human ATR) in a manner that is distinct from its role in checkpoint control. Here, we show that *rad3 rqh1* mutants are normally committed to a lethal pathway of DNA repair requiring homologous recombination, but blocking this pathway by Rhp51 inactivation restores viability. Remarkably, viability is also restored by overexpression of Cut8, a nuclear envelope protein involved in tethering and proper function of the proteasome. In keeping with a recently described function of the proteasome in the repair of DNA double-strand breaks, we found that Cut8 is also required for DNA double-strand break repair and is essential for proper chromosome segregation in the absence of Rqh1, suggesting that these proteins might function in a common pathway in homologous recombination repair to ensure accurate nuclear division in *S. pombe*.**

Eukaryotic cells engage a variety of protective responses following DNA damage. These include enzymes which repair specific DNA lesions after DNA damage as well as regulators that coordinate DNA repair and cell cycle progression. Mutations abolishing many of these processes result in genome instability and cause cancer-prone syndromes in humans. One important class of these syndromes is caused by defects in RecQ helicases (1). These enzymes unwind DNA in a 3' to 5' direction and are proposed to function in DNA recombination repair. Another example of this is the phosphatidylinositol 3-kinase-like protein kinases ATM (mutated in ataxia telangiectasia) (12) and ATR (ATM and Rad3 related). These proteins are associated with DNA damage surveillance and control of cell cycle checkpoints. Three checkpoint protein complexes have been suggested to play roles in sensing DNA damage. The components of these complexes in *Schizosaccharomyces pombe* are the checkpoint Rad proteins, including the Rad3-Rad26 complex (human ATR and ATRIP, respectively), the PCNA-like Rad9-Rad1-Hus1 (9-1-1) complex, and the Rad17-replication factor C clamp loader complex (4). They are involved in the activation of two downstream effector kinases, Chk1 and Cds1 (19, 29). The Cds1-dependent S-phase checkpoint is required for arresting the cell cycle, stabilizing replication forks, and preventing late origin firing. The Chk1-dependent DNA damage checkpoint prevents entry into mitosis until the completion of DNA repair.

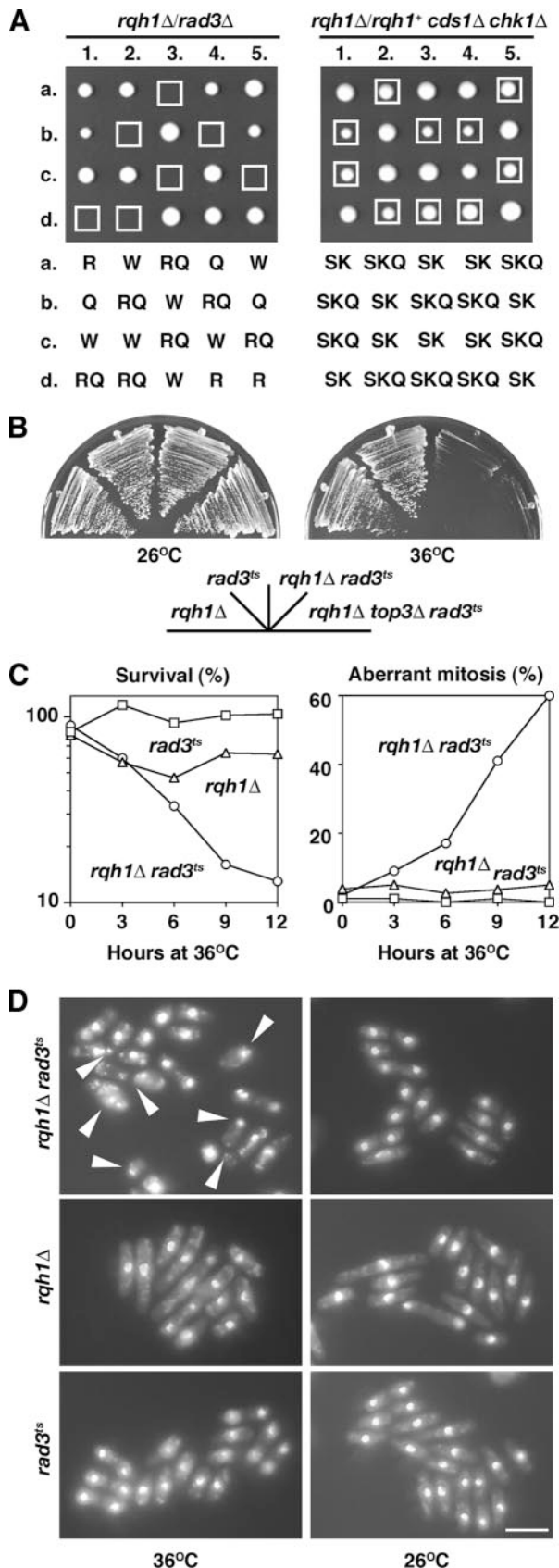
DNA double-strand breaks (DSBs) are the most severe damage to DNA caused by environmental factors and occur

spontaneously during normal cellular metabolism. In eukaryotes, DSBs are repaired by homologous recombination (HR) or nonhomologous end-joining (NHEJ) mechanisms (22). In both *Schizosaccharomyces pombe* and *Saccharomyces cerevisiae*, HR is the preferred pathway for DSB repair and is under the control of the *RAD52* epistasis group of genes, including *rhp51*⁺ (*RAD51* homolog) (25). Proteins belonging to the RecQ helicase family, such as *S. pombe* Rqh1, *S. cerevisiae* Sgs1, and human BLM (mutated in Bloom's syndrome), appear to play a role in DNA recombination repair at a later step. Interestingly, Sgs1, Rqh1, and BLM form functional enzyme complexes with DNA topoisomerase III (3, 14, 33). In vitro studies have also shown that RecQ-like helicase and TopIII can act together to resolve double Holliday junction structures, which probably constitute a late recombination intermediate (34). RecQ helicases may also function to disrupt potential substrates for HR by preventing replication fork collapse, thus preventing high levels of recombination and ensuring subsequent fidelity of chromosome segregation (32). Additional factors required for DSB repair include *S. cerevisiae* Sem1, a 19S proteasome lid subunit and an ortholog of human DSS1, which binds the breast cancer susceptibility protein BRAC2 (9). Chromatin immunoprecipitation showed that Sem1 is recruited along with the 19S and 20S proteasome subcomplexes to a DSB in vivo, and this recruitment is dependent on components of both the HR and NHEJ repair pathways, suggesting a direct role of the proteasome in DSB repair (13).

Previously, we and another group identified a specific interaction between Rqh1-Top3 and Rad3 (20, 31). In this study, we further extend these findings and show that *rad3 rqh1* mutants are normally committed to a lethal pathway of DNA repair

* Corresponding author. Mailing address: Department of Zoology, South Parks Road, Oxford OX1 3PS, United Kingdom. Phone: 44 1865 271212. Fax: 44 1865 271192. E-mail: shaowin.wang@zoo.ox.ac.uk.

[∇] Published ahead of print on 18 December 2006.



requiring HR, but blocking this pathway by Rhp51 inactivation restores viability. We describe a function of Cut8 in DSB repair that is required for the survival of *rqh1* mutants when Rad3 is also inactivated. Cut8 is a nuclear envelope protein involved in proteasome tethering and its proper function (26, 27). These results are consistent with a direct role of the proteasome in DSB repair (13), and the proteasome might function with other proteins in a common pathway in HR repair to ensure accurate nuclear division in *S. pombe*.

MATERIALS AND METHODS

Fission yeast strains and methods. We constructed all strains according to standard procedures (18). The original *cut8* (27), *gar2-GFP* (23), *rad22-CFP* (6), *slx1* (5), and checkpoint mutants (16) were gifts from M. Yanagida, M. Yamamoto, P. Russell, and A. M. Carr, respectively. The strains used for this study were HM123 (*h⁻ leu1*), SW1040 (*h⁻ rqh1::ura4⁺ ura4*), SW347 (*h⁻ rqh1::kan^r ade6 leu1 ura4 his7*), SW364 (*h⁻ cds1::ura4 chk1::ura4 ade6 leu1 ura4*), SW369 (*h⁻ rqh1::kan^r cds1::ura4 chk1::ura4 ade6 leu1 ura4*), SW365 (*h⁻ rad3^{ts} ade6 leu1 ura4*), SW286 (*h⁻ rad3^{ts} rqh1::ura4 ade6 leu1 ura4*), SW167 (*h⁻ rad3^{ts} rqh1::kan^r top3::ura4 ade6 leu1 ura4*), SW253 (*h⁻ cut8::ura4 leu1 ura4*), SW1267 (*h⁻ rad22-2CFP::kan^r leu1 ura4*), SW1237 (*h⁻ cut8::ura4 rad22-2CFP::kan^r leu1 ura4*), SW1305 (*h⁻ rad3^{ts} rad22-2CFP::kan^r leu1 ura4*), SW1307 (*h⁻ rad3^{ts} rqh1::ura4 rad22-2CFP::kan^r leu1 ura4*), SW302 (*h⁻ cut8-HA::LEU2 leu1*), SW724 (*h⁺ cut8-HA::LEU2 rad3::ura4 leu1 ura4*), SW303 (*h⁻ cut8-GFP::LEU2 leu1*), SW722 (*h⁺ cut8-GFP::LEU2 rad3::ura4 ade6 leu1 ura4*), SW259 (*mat1Δ17::LEU2 rqh1::kan^r rhp51::ura4 ade6 leu1 ura4*), SW845 (*mat1M-mst0 rad3::LEU2 ade6 leu1 ura4*), SW880 (*mat1M-mst0 rad3::LEU2 rqh1::kan^r rhp51::ura4 ade6 leu1 ura4 his7*), SW773 (*mat1Δ17::LEU2 rhp51::kan^r rad3::ura4 ade6 leu1 ura4*), SW213 (*mat1Δ17::LEU2 rhp51::ura4 ade6 leu1 ura4*), SW1387 (*mat1M-mst0 rqh1::kan^r rhp54::ura4 ade6 leu1 ura4*), SW1386 (*mat1M-mst0 rad3::LEU2 rqh1::kan^r rhp54::ura4 ade6 leu1 ura4*), SW1383 (*mat1M-mst0 rhp54::ura4 rad3::LEU2 ade6 leu1 ura4*), SW1373 (*h⁺ rhp54::ura4 ade6 leu1 ura4*), SW1381 (*mat1Δ17::LEU2 rqh1::kan^r rhp55::ura4 ade6 leu1 ura4*), SW1391 (*mat1M-mst0 rad3::LEU2 rqh1::kan^r rhp55::ura4 ade6 leu1 ura4*), SW1392 (*mat1Δ17::LEU2 rhp55::ura4 rad3::LEU2 ade6 leu1 ura4*), SW1384 (*mat1Δ17::LEU2 rhp55::ura4 ade6 leu1 ura4*), SW1388 (*h⁺ cut8::ura4 rad3::LEU2 ade6 leu1 ura4*), SW1385 (*h⁻ cut8::ura4 rhp51::LEU2 ade6 leu1 ura4*), SW1389 (*h⁻ rqh1::kan^r cut8::ura4 rhp51::LEU2 ade6 leu1 ura4*), SW1390 (*h⁺ slx1::kan^r cut8::ura4 rhp51::LEU2 ade6 leu1 ura4*), SW1204 (*h⁺ slx1::kan^r leu1 ura4*), SW990 (*h⁻ rad9::ura4 gar2-GFP::kan^r leu1 ura4*), and SW885 (*h⁺ rad3::LEU2 gar2-GFP::kan^r ade6 leu1 ura4*).

FIG. 1. Rad3 is required for the survival of *rqh1Δ* cells. (A) Five tetrads derived from diploid *h⁺/h⁻ rqh1::kan^r/rqh1⁺ rad3::ura4⁺/rad3⁺* (left) and *rqh1::kan^r/rqh1⁺ cds1::ura4⁺/cds1::ura4⁺ chk1::ura4⁺/chk1⁺ ura4⁺* (right) strains were microdissected onto yeast extract (YE) agar, and the resulting colonies were photographed after 5 days of growth at 30°C. The genotypes of the segregants were determined by replica plating and are indicated schematically (W, *rqh1⁺ rad3⁺*; R, *rad3Δ*; Q, *rqh1Δ*; S, *cds1Δ*; K, *chk1Δ*). Boxes indicate the positions of *rqh1 rad3* double (left) and *rqh1 cds1 chk1* triple (right) mutants. (B) The strains, as indicated, were streaked in parallel onto YE agar plates and photographed after 3 days of incubation at 26°C or 36°C, as indicated. (C) The strains, as indicated, were grown in liquid culture to mid-logarithmic phase at 26°C and shifted to 36°C, the restrictive temperature. Samples of 500 cells taken at the indicated times after the shift to 36°C were plated in duplicate onto YE agar and incubated at 26°C. After 5 days of growth, viability was scored as a percentage of the number of colonies formed by the sample taken at time zero. Samples taken at the same time points were fixed, DAPI stained, and examined by fluorescence microscopy. The percentage of each sample exhibiting aberrant mitosis was scored as a total of at least 200 cells for each time point. (D) Fluorescence micrographs show representative fields of DAPI-stained cells of the indicated strains grown at 26°C (right panels) or 9 h after the shift to 36°C (left panels). Cells exhibiting aberrant mitosis are indicated (arrowheads). Bar, 10 μm.

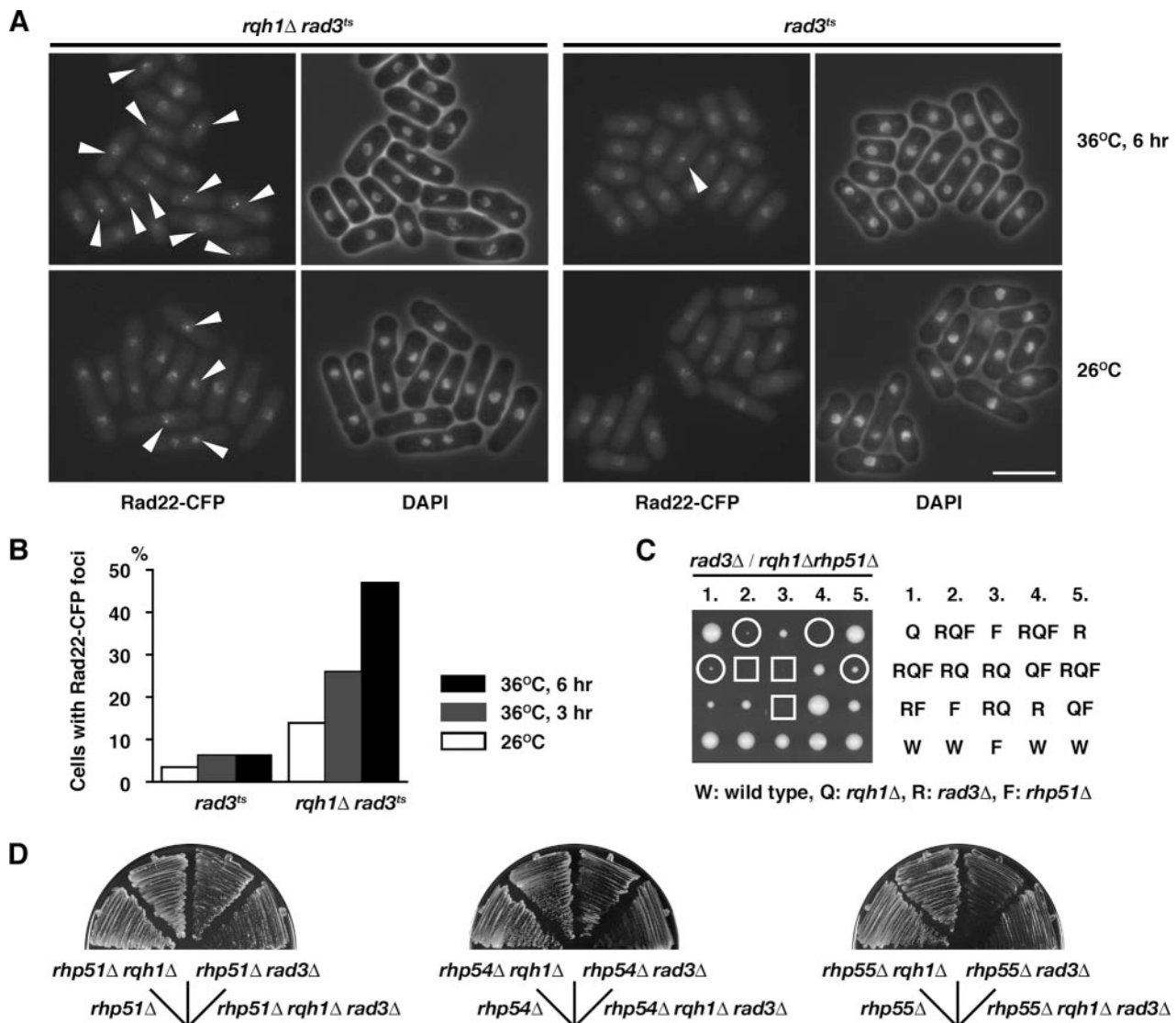


FIG. 2. Inactivation of HR suppresses *rad3 rqh1* synthetic lethality. (A) Fluorescence micrographs showing Rad22-cyan fluorescent protein (CFP) localization in *rad3^{ts}* and *rqh1Δ rad3^{ts}* cells grown at 26°C or 6 h after the shift to 36°C. Bar, 10 μ m. (B) The percentages of cells with Rad22 foci in each strain are shown. (C) Five tetrads derived from the diploid *mat1PΔ17::LEU2/mst0 rqh1::kan⁺/rqh1⁺ rhp51::ura4⁺/rhp51⁺ rad3::LEU2/rad3⁺* strain were microdissected onto yeast extract (YE) agar, and the resulting colonies were photographed after 5 days of growth at 30°C. The genotypes of the segregants were determined by replica plating and are indicated schematically (W, *rqh1⁺ rad3⁺ rhp51⁺*; Q, *rqh1Δ*; R, *rad3Δ*; F, *rhp51Δ*). The positions of *rqh1 rad3* double mutants (boxes) and *rqh1 rad3 rhp51* triple mutants (circles) are indicated. (D) The strains, as indicated, were streaked in parallel onto YE agar plates. Plates were photographed after 3 days of incubation at 30°C.

cDNA library screen and plasmids. The *rqh1Δ rad3^{ts}* strain was transformed with an *S. pombe* cDNA library (30) constructed in the vector pREP3X, a *LEU2*-containing multicopy plasmid. The *leu⁺* transformants (5×10^5) obtained were tested for their temperature sensitivity. Cells capable of forming colonies at 36°C were isolated. The plasmids recovered from these transformants were sequenced using an ABI sequencer and ABI PRISM dRhodamine reagents (Applied Biosystems). Plasmid *pcut1* containing the full *cut1* genomic sequence was isolated by complementation cloning of a *cut1-206* mutation with the pUR library (2). Plasmid *pcut2* and *pcdc13* (under the control of the *nmu41* promoter) were kindly provided by E. C. Chang (35).

Immunocytochemistry and microscopy. Cell extracts were prepared by trichloroacetic acid precipitation, and immunoblotting was performed as previously described (31). The mouse anti-influenza hemagglutinin (HA) monoclonal antibody HA-11 (Babco, Berkeley, CA) was used for the detection of HA-tagged Cut8 proteins. Cdc2 was detected using the mouse monoclonal antibody Y100 (generated by J. Gannon and kindly provided by H. Yamano). Cells fixed in 70%

ethanol or methanol for green fluorescent protein (GFP) were rehydrated and stained with 4',6'-diamidino-2-phenylindole (DAPI) before examination by fluorescence microscopy as previously described (31).

Pulsed-field gel electrophoresis. DNA plugs were prepared as previously described (31). Pulsed-field gel electrophoresis was carried out with a 0.8% chromosomal grade agarose gel in 1 \times TAE buffer (40 mM Tris-acetate, 2 mM EDTA) by using a CHEF III apparatus (Bio-Rad, Hercules, CA). The settings were as follows: 2 V/cm; switch time, 30 min; angle, 106°; 14°C; 48 h.

RESULTS

Synthetic lethality in *rqh1Δ rad3Δ* double mutants. It was previously found that the *rqh1Δ* mutant caused synthetic lethality in *rad3Δ* and *rad26Δ* mutants but not in other check-

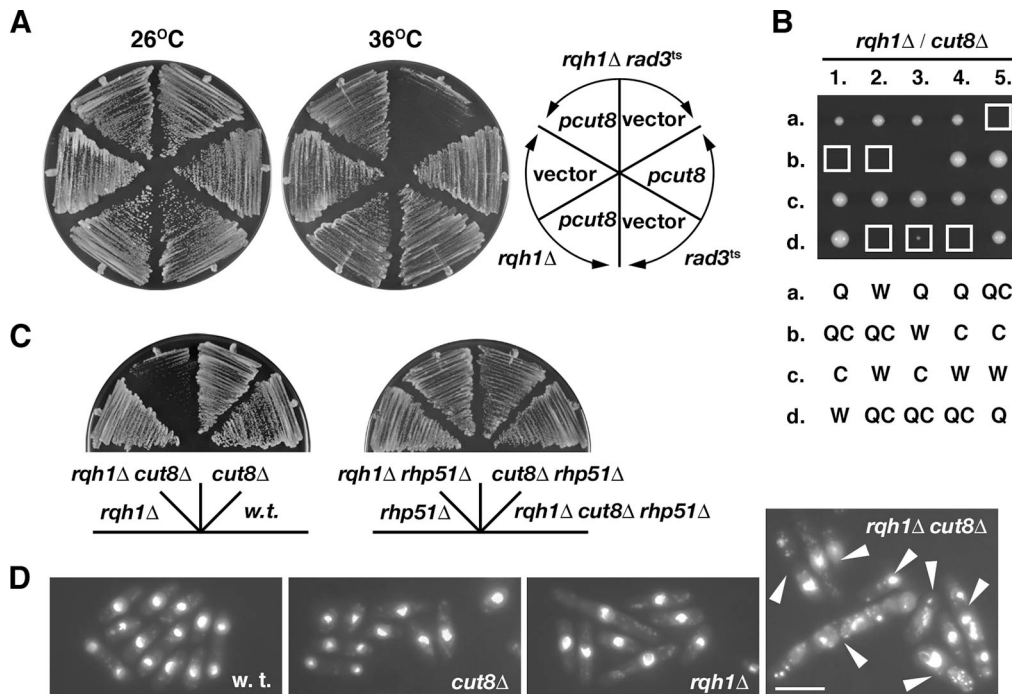


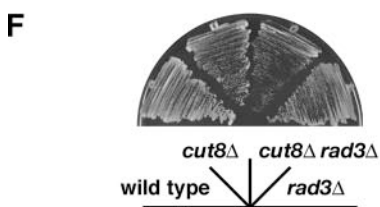
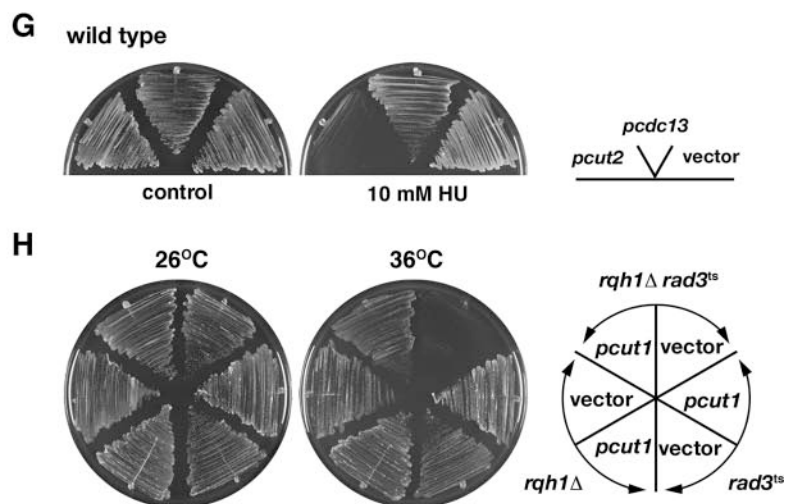
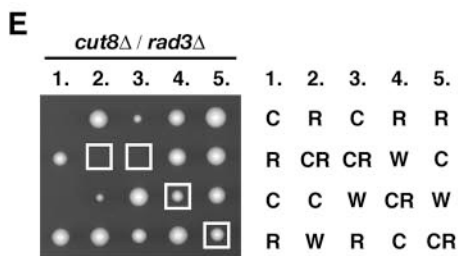
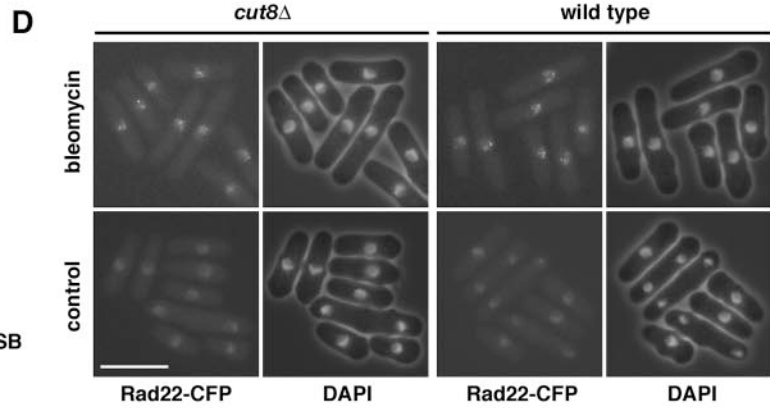
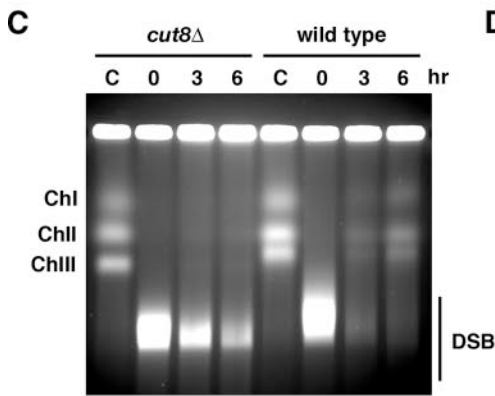
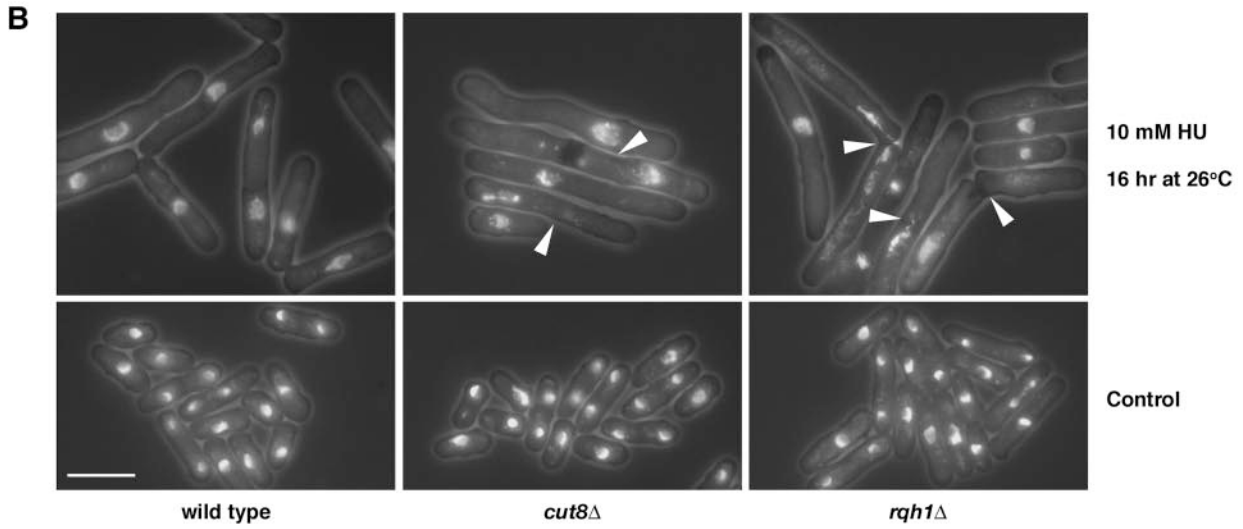
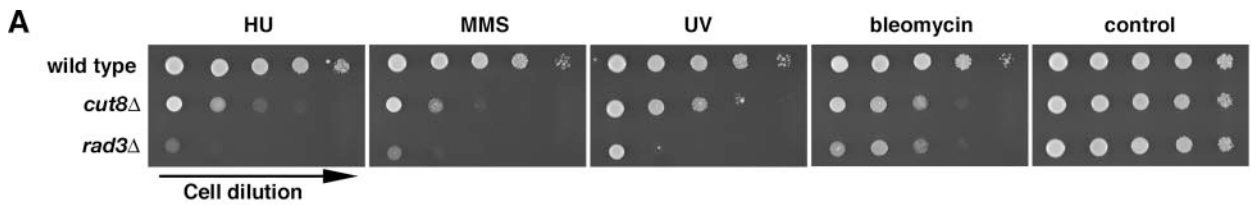
FIG. 3. Cut8 is required for the survival of *rqh1Δ* cells. (A) The strains, as indicated, containing plasmid *pcut8* or empty vector were streaked in parallel onto Edinburg minimal medium agar plates. Plates were photographed after 3 days of incubation at 26°C and 36°C, as indicated. (B) Five tetrads derived from the diploid h^+/h^- *rqh1::kan^r/rqh1^+* *cut8::ura4^+/cut8^+* strain were microdissected onto yeast extract (YE) agar, and the resulting colonies were photographed after 5 days of growth at 26°C. The genotypes of the segregants were determined by replica plating and are indicated schematically (W, *rqh1^+ cut8^+*; Q, *rqh1Δ*; C, *cut8Δ*). Boxes indicate the position of the *rqh1* double mutant with *cut8*. (C) The strains, as indicated, were streaked in parallel onto YE agar plates and photographed after 3 days of incubation at 26°C. (D) Fluorescence micrographs show representative fields of DAPI-stained cells of the indicated strains grown at 26°C. Cells exhibiting aberrant mitosis are indicated (arrowheads). Bar, 10 μm. w.t., wild type.

point mutants, affecting the checkpoint sliding clamp (*rad9*, *rad1*, and *hus1*) or clamp loader *rad17* (20). This indicates that *rad3* together with *rad26* might have a function in addition to their role in checkpoint control that is required for the survival of *rqh1Δ* mutants. This interpretation is further substantiated by the fact that simultaneous deletion of the two downstream effector kinases, Chk1 and Cds1, has no detrimental effect on the growth of *rqh1Δ* cells (Fig. 1A). Similar results have been found for *top3* mutants. Consistent with the genetic interaction between *top3* and *rqh1*, the *top3* mutant is synthetically lethal in combination with *rad3Δ* or *rad26Δ* mutants but not with other checkpoint mutants (31).

To examine the basis of the growth defect in the *rqh1 rad3* double mutant, we created a conditional mutant combining a *rad3* temperature-sensitive (*ts*) mutation (16) with the *rqh1* deletion. The *rqh1Δ rad3^{ts}* double mutant grew at 25°C but was unable to grow at 36°C, whereas single parental mutants remained fully viable at both temperatures (Fig. 1B). Given that deletion of *rqh1* suppresses lethality in *top3* mutants, we tested an *rqh1Δ top3Δ rad3^{ts}* triple mutant for viability and found that it is not viable at the restrictive temperature. These results suggest that the synthetic lethality between *rqh1Δ* and *rad3Δ* mutants is not due to inappropriate regulation of topoisomerase III activity. Examination of nuclear morphology revealed that the loss of viability in *rqh1Δ rad3^{ts}* cells correlates with defective mitoses, in which septation occurs without proper chromosome segregation (Fig. 1C and D). Given that simulta-

neous deletion of the two downstream effector kinases, Chk1 and Cds1, has no detrimental effect on the growth of *rqh1Δ* cells, these results suggest that the growth defect in the *rqh1 rad3* double mutant arises from the failure to process DNA damage, which is manifested upon entry into mitosis as aberrant chromosome segregation. The fact that the viability drops steadily over 12 h, as seen in *top3* mutants, suggests that the lethality is due to spontaneous damage caused by the loss of Rqh1 or Rad3 functions.

Inactivation of HR suppresses *rad3 rqh1* synthetic lethality. One possible explanation for the lethality of the *rqh1 rad3* double mutant is that DNA damage lesions are processed via a pathway dependent on HR, but intermediates are not properly resolved, leading to chromosome segregation defects and lethality. To examine this possibility, we analyzed the formation of Rad22 (ScRad52) foci, which allows the identification of subnuclear sites where recombination proteins are loaded onto DNA (6). Following the inactivation of Rad3, the number of *rqh1Δ* cells with Rad22 foci increases (Fig. 2A and B), consistent with either an increased rate of HR or a block in the recombination pathway. To examine how the inactivation of HR affected the *rqh1 rad3* mutant, we introduced an *rhp51* deletion (*ScRAD51*) into this mutant background (Fig. 2C and D). We performed the tetrad analysis using *mat1PΔ17::LEU2* and *smt0* mutations that abolish the formation of a DSB at *mat1* and suppress the undesired growth defects in *rad3Δ rhp51Δ* mutants (10). Analysis of spore colonies indicated that while no



rad3Δ rqh1Δ progeny was recovered, as expected from previous results, several *rad3Δ rqh1Δ rhp51Δ* triple mutants grew into small- or intermediate-sized colonies that could be propagated. Similar results were observed with the other *RAD52* epistasis group mutants, although the *rhp54* and *rhp55* triple mutants grew more slowly than the *rhp51* mutant (Fig. 2D). Taken together, these results suggest that *rad3 rqh1* mutants are normally committed to a lethal pathway of DNA repair requiring HR, but blocking this pathway restores viability.

Cut8 is required for the survival of *rqh1Δ* cells. To learn more about the defects in *rqh1 rad3* double mutants, we screened for genes capable of suppressing *rqh1Δ rad3^{ts}* lethality when overexpressed (Fig. 3A). In this way, *cut8⁺*, which encodes a nuclear envelope protein involved in proteasome tethering (26, 27), was identified. The specificity of this interaction is further substantiated by synthetic lethality of a strain carrying both *cut8* and *rqh1* deletions (Fig. 3B). After prolonged incubation, *cut8Δ rqh1Δ* spores germinated (Fig. 3C), but these cells were very slowly growing and generally highly elongated with extensive nuclear DNA fragmentation (Fig. 3D). As with the genetic interaction between *rad3* and *rqh1*, *cut8* and *rqh1* synthetic lethality was suppressed by deletion of *rhp51* (Fig. 3C).

Cut8 is required for DNA repair. Further experiments were performed to determine the role of Cut8 in Rqh1 deficiency. Consistent with the results described above, we found that *cut8Δ* mutants are hypersensitive to the ribonucleotide reductase inhibitor hydroxyurea (HU) in addition to DNA-damaging agents (26) (Fig. 4A). This sensitivity is not due to checkpoint defects, as *cut8Δ* mutants, like wild-type cells and unlike *rad3Δ* mutants, could arrest cell cycle progression and became highly elongated in response to HU and bleomycin, a radiomimetic drug that causes DSBs (Fig. 4B and data not shown). We thus investigated whether *cut8Δ* cells were able to repair DSBs efficiently by using pulsed-field gel electrophoresis to follow repair after exposing cells to bleomycin (Fig. 4C). After bleomycin treatment, chromosomes were damaged as shown by the low-molecular-weight smear of DNA. Fragmented chromosomes were mostly rejoined in wild-type cells by 3 h, but in contrast, chromosomes in the *cut8Δ* mutant remained fragmented even after 6 h. Thus, *cut8Δ* cells are defective in DSB repair.

In cycling *S. pombe* cells, HR is the dominant pathway for DSB repair whereas NHEJ is dispensable for cell survival (7). To explore the role of Cut8 in DNA repair, we examined the formation of Rad22 (ScRad52) foci in *cut8Δ* mutants. As shown in Fig. 4D, the rapid formation of Rad22 foci in response to bleomycin treatment occurred in wild-type cells as well as *cut8Δ* mutants, indicating that the initial recruitment of Rad22 is independent of Cut8. Taken together, these results suggest that Cut8 is required for the completion but not the initiation of HR repair. Like the *rhp51* mutant, the *cut8* mutant is viable in combination with *rad3* mutation (Fig. 4E and F).

Cut1 and Cut2 in Rqh1-associated defects. The results presented above suggest a function of *cut8⁺* in DNA damage but do not clarify the molecular basis of this defect. The degradation of two proteins, namely, the mitotic cyclin Cdc13 and the securin Cut2, is dramatically delayed in a *cut8* mutant, and this is apparently due to the mislocalization of the proteasome (26). It is not obvious why a delay in Cdc13 degradation would lead to a defect in DNA repair, but misregulation of cohesin cleavage, via Cut2, could be relevant since cohesin has been implicated in DSB repair in a number of studies (11). In particular, Nagao et al. (21) showed that cleavage of cohesin/Rad21 by separase/Cut1 is needed for efficient DNA repair, and this could be related to the enhanced loading of cohesin that is seen at DSBs (24, 28). Since Cut1 is regulated by the securin Cut2, it is possible that the proper function of cohesin in DNA damage repair is aberrant if Cut2 degradation is defective. To test this, we overexpressed *cut2⁺* and also *cut13⁺* in wild-type cells and examined their ability to form colonies on plates containing HU. As shown in Fig. 4G, cells overexpressing *cut2⁺* were unable to grow at the concentration of HU that allowed colony formation in the control strain or cells overexpressing *cut13⁺*. We also tested the effects of Cut1 overexpression, since this might have similar effects to the promotion of Cut2 degradation by overexpression of Cut8. Indeed, as shown in Fig. 4H, overexpression of *cut1⁺* suppressed the temperature sensitivity of *rqh1Δ rad3^{ts}* cells. Taken together, these results suggest that Cut8 functions in a common pathway with Cut2 and Cut1 in the cellular response to HU inhibition of DNA replication as well as DNA damage that is important for cell survival in the absence of Rqh1.

FIG. 4. Cut8 is required for DNA repair. (A) Tenfold serial dilutions of the indicated strains spanning the range from 10^6 to 10^2 cells were spotted onto yeast extract (YE) agar containing 5 mM HU, 0.005% methyl methanesulfonate (MMS), 5 μ g/ml bleomycin, or no drug (control). "UV" cells were exposed to 150 J/m² UV-C. Plates were photographed after 3 to 5 days of incubation at 26°C. (B) Fluorescence micrographs showing *cut8Δ* and *rqh1Δ* cells after incubation at 26°C in the presence of 10 mM HU for 16 h or no drug. Cells exhibiting aberrant mitosis are indicated (arrowheads). Bar, 10 μ m. (C) Pulsed-field gel electrophoresis analyses of chromosomes (Ch) from bleomycin-treated cells. Equal numbers of cells were prepared in agarose gel plugs from exponentially growing cultures of the indicated strains following bleomycin treatment (5 μ g/ml bleomycin at 26°C for 1 h). Cells were harvested at the time of bleomycin addition ("C") and at 3-h intervals after the removal of bleomycin for up to 6 h. Pulsed-field gel electrophoresis was carried out as described in Materials and Methods. (D) Fluorescence micrographs showing Rad22-cyan fluorescent protein (CFP) localization in wild-type and *cut8Δ* cells after incubation at 26°C in the presence of 10 μ g/ml bleomycin for 1 h or no drug (control). Bar, 10 μ m. (E) Five tetrads derived from the diploid *h⁺/h⁻ cut8::ura4⁺/cut8⁺ rad3::LEU2/rad3⁺* strain were microdissected onto YE agar, and the resulting colonies were photographed after 5 days of growth at 26°C. The genotypes of the segregants were determined by replica plating and are indicated schematically (W, *cut8⁺ slx1⁺*; C, *cut8Δ*; R, *rad3Δ*). Boxes indicate the position of the *cut8* double mutant with *rad3*. (F) The strains, as indicated, were streaked in parallel onto YE agar plates and photographed after 3 days of incubation at 26°C. (G) Wild-type strains containing the indicated plasmids under the control of the *nmt41* promoter were streaked in parallel onto Edinburgh minimal medium (EMM) agar containing 10 mM HU or no drug (control). Plates were photographed after 3 days of incubation at 30°C. (H) The strains, as indicated, containing plasmid *pcut1* or empty vector were streaked in parallel onto EMM agar plates. Plates were photographed after 3 days of incubation at 26°C and 36°C, as indicated.

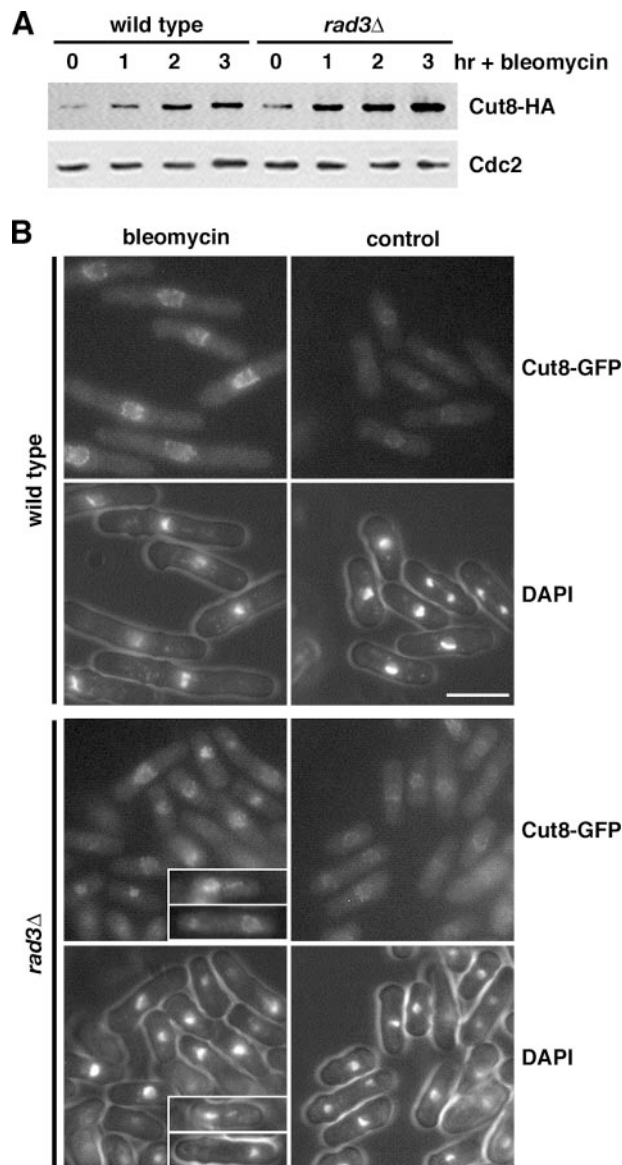


FIG. 5. Accumulation of Cut8 in response to DNA damage. (A) Bleomycin (10 μ g/ml) was added to asynchronous cultures of wild-type and *rad3Δ* cells that expressed the chromosomally integrated Cut8-HA gene under the native promoter growing at 26°C in yeast extract medium. Cells harvested at hourly intervals were processed for immunoblotting using antibodies against HA. Antibodies against Cdc2 were used as controls. (B) Fluorescence micrographs showing Cut8-GFP localization in wild-type and *rad3Δ* cells after incubation at 26°C in the presence of 10 μ g/ml bleomycin for 3 h or no drug (control). Bar, 10 μ m. Note that unlike wild-type cells, which became highly elongated in response to bleomycin treatment, *rad3Δ* cells failed to arrest cell cycle progression and displayed the “cut” phenotype, as shown in the insets.

Accumulation of Cut8 in response to DNA damage. Next, we examined how Cut8 responds to DNA damage and found that the protein level increased dramatically in wild-type cells after the addition of bleomycin (Fig. 5A). A more dramatic increase was seen in a *rad3Δ* mutant, indicating that this accumulation is independent of Rad3. This is not due to an indirect effect of cell cycle arrest, as *rad3* mutants, unlike wild-type cells, pro-

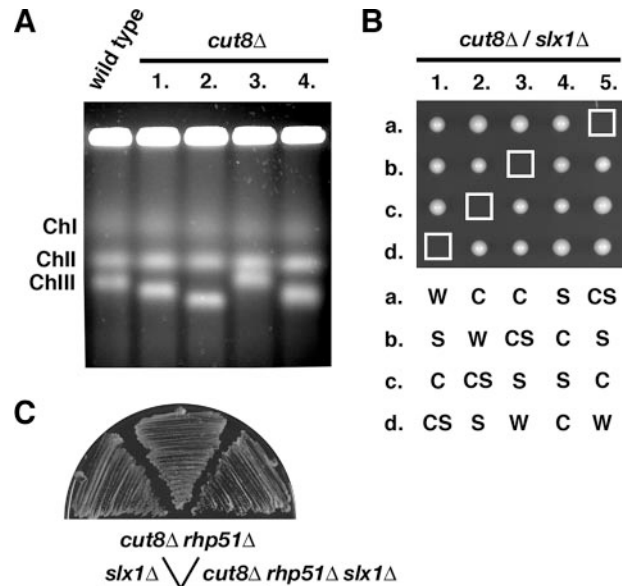


FIG. 6. Cut8 is important for rDNA maintenance. (A) Pulsed-field gel electrophoresis analyses of chromosomes (Ch) from *cut8Δ* mutants. Equal numbers of cells were prepared in agarose gel plugs from exponentially growing cultures of wild-type or *cut8Δ* cells (four independent isolates). Pulsed-field gel electrophoresis was carried out as described in Materials and Methods. (B) Five tetrads derived from the diploid $h^+/h^- cut8::ura4^+/cut8^+ slx1::kan^+/slx1^+$ strain were microdissected onto yeast extract (YE) agar, and the resulting colonies were photographed after 5 days of growth at 26°C. The genotypes of the segregants were determined by replica plating and are indicated schematically (W, *cut8*⁺ *slx1*⁺; C, *cut8Δ*; S, *slx1Δ*). Boxes indicate the position of the *cut8* double mutant with *slx1*. (C) The strains, as indicated, were streaked in parallel onto YE agar plates and photographed after 3 days of incubation at 26°C.

ceed with cell cycle progression regardless of DSBs generated by bleomycin (Fig. 5B), and in any case, Cut8 levels are constant during the cell cycle (data not shown). We also examined the cellular localization of GFP-tagged Cut8. Cut8 is enriched in the nucleus, particularly at the nuclear periphery after the addition of bleomycin (Fig. 5B), in keeping with its function in promoting the nuclear enrichment of the proteasome (26, 27).

Cut8 is important for rDNA maintenance. During the course of analysis of the chromosome structure in *cut8Δ* mutants, we consistently observed anomalous migration of chromosome III from *cut8Δ* cells, which had a significantly faster mobility than the wild-type chromosome (Fig. 6A, lanes 1, 2, and 4). Similar results were recently described for *rqh1* and *top3* mutants, in which the reduction of chromosome III length is caused by the loss of ribosomal DNA (rDNA) repeats (5, 31). Consistent with the genetic interaction between *cut8* and *rqh1*, these results suggest that Cut8 might have a role in the maintenance of the rDNA repeats located at the ends of chromosome III. This was further supported by the genetic interaction between *cut8*⁺ and *slx1*⁺, which encodes a structure-specific endonuclease that maintains rDNA copy number (5). As shown in Fig. 6B, similar to that in *rqh1Δ* mutants, the deletion of *cut8* resulted in synthetic lethality in *slx1Δ* mutants, probably due to the failure to repair stalled replication forks in rDNA loci. Furthermore, *cut8 slx1* synthetic lethality was sup-

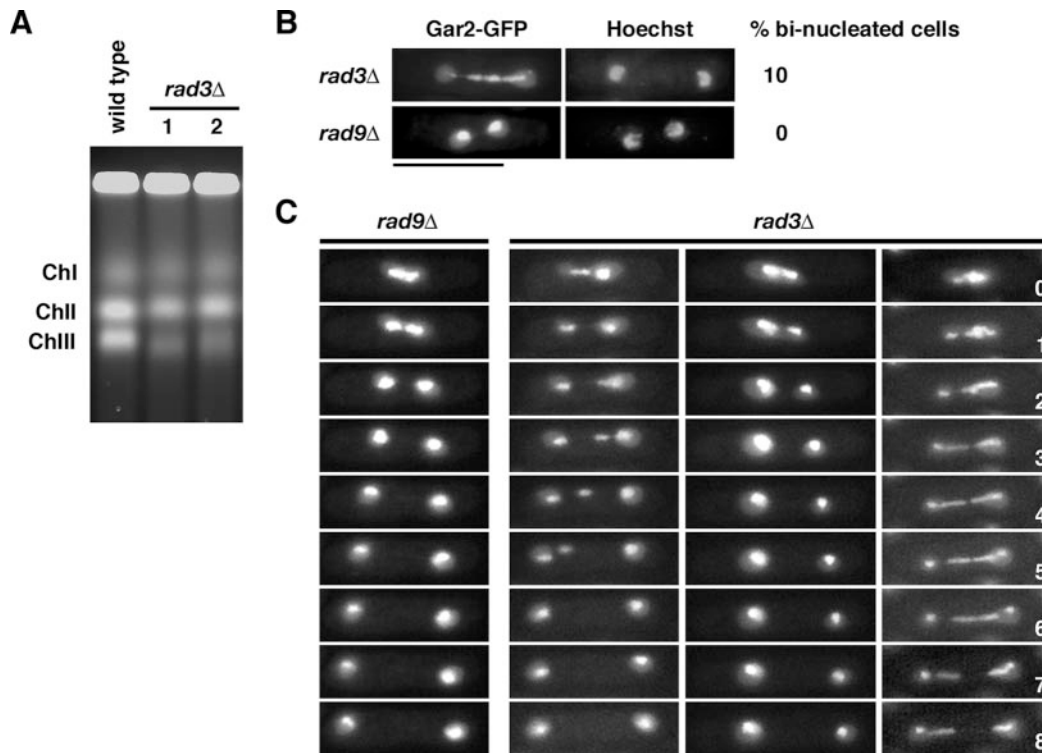


FIG. 7. *rad3* mutants are defective in nucleolar segregation. (A) Pulsed-field gel electrophoresis analyses of chromosomes (Ch) from *rad3Δ* mutants. Equal numbers of cells were prepared in agarose gel plugs from exponentially growing cultures of wild-type or *rad3Δ* cells (two independent isolates). Pulsed-field gel electrophoresis was carried out as described in Materials and Methods. (B) Fluorescence micrographs showing Gar2-GFP and DNA (Hoechst 33342) localization in living *rad3Δ* and *rad9Δ* cells. The percentages of binucleated cells displaying aberrant nucleolar structures in each strain are shown ($n = 200$). Bar, 10 μm . (C) Visualization of lagging Gar2-GFP signal in *rad3Δ* cells. Individual cells of the indicated strains expressing Gar2-GFP were observed as in panel B, over an 8-minute period, with images collected every minute.

pressed by the deletion of *rhp51*, in keeping with the genetic interaction between *cut8* and *rqh1* (Fig. 6C).

Rad3 is required for proper segregation of rDNA. Having established that Cut8 has a role in rDNA maintenance, we were interested to see whether Rad3 plays a role in the maintenance of rDNA structure. As shown in Fig. 7A, we consistently observed anomalous migration of chromosome III from *rad3Δ* cells, which also showed a greater reduction in the intensity of signal than chromosome I or II (40% reduction compared with that of wild-type cells), perhaps indicating the accumulation of abnormal structures that cannot enter the gel. This was further explored by examining the segregation of rDNA in *rad3Δ* cells by using a fusion protein between GFP and the nucleolar protein Gar2, which localizes to the rDNA where transcription occurs (23). Although not extremely frequent, abnormal anaphase progression, monitored in living cells by Gar2-GFP fluorescence, was observed in 10% of binucleated cells ($n = 200$) (Fig. 7B). In some *rad3Δ* cells, this took the form of two unequal masses of Gar2-GFP (Fig. 7C, middle panels). In other cells, an extended bridge of Gar2-GFP often persisted for some time between the nascent daughter nuclei (Fig. 7C, right panels), as previously described for *rqh1* and *top3* (31, 32), but this was not observed in wild-type cells or checkpoint mutants, such as the *rad9Δ* mutant. Taken together, these results suggest that Rad3 is required for the proper segregation of rDNA.

DISCUSSION

Two main points emerge from our analysis of *rad3* and *rqh1*. First, consistent with the independent assembly of different checkpoint protein complexes in response to DNA damage, our results suggest that Rad3 regulates more proteins than the checkpoint effectors and might directly participate in repair activity. Secondly, we describe a function of Cut8 in DSB repair that is required for cell survival in the absence of Rqh1. We also present evidence that these proteins function in a common pathway in HR repair that is essential for ensuring fidelity of chromosome segregation.

The results presented here, together with our previous data on the interaction between *rqh1* and *top3*, suggest that Rqh1-Top3 has a function that is essential for accurate chromosome segregation (31, 32). Rqh1, with Top3, is presumably required to process or disrupt aberrant recombination structures that arise during S phase to allow proper chromosome segregation during mitosis. Intriguingly, in the absence of Rqh1, the processing of these structures appears to be dependent on Rad3 in a manner that is distinct from its role in checkpoint control. In *S. cerevisiae*, the ATR homolog Mec1, together with Rad53 (Cds1 homolog), has been implicated in facilitating DNA replication by stabilizing replication forks (15). However, the requirement of Rad3 function in the absence of Rqh1 is independent of Cds1, suggesting that it acts through a different pathway. Like mammalian ATM/

ATR, Rad3 might have an additional function in the regulation of DNA damage repair (8), and consistent with this, we identified *cut8*, which is required for DSB repair, as a multicopy suppressor of *rqh1 rad3* synthetic lethality. The growth defects in *rqh1 rad3* mutants could arise from the failure to process certain DNA lesions, such as an unresolved recombination intermediate from a collapsed replication fork (34). Entering mitosis with sister chromatids entangled by unresolved recombination intermediates would impair subsequent chromosome segregation. This hypothesis is further supported by the fact that the inactivation of HR by the deletion of *rhp51* is able to suppress the lethality of *rad3Δ* *rqh1Δ* mutants, suggesting a function of Rad3 in repair dependent on HR. Consistent with this interpretation, Mochida and Yanagida (17) recently showed that Rad3 was needed for the repair of DSBs after UV irradiation in cells arrested at G₀ as well as G₂ phase. Also, Nagao et al. (21) showed that modification of the cohesin subunit Rad21 by Rad3 might be involved in the recognition of damaged lesions that must be repaired. In line with our analysis of *rad3* and *rqh1*, phosphorylation of Rad21 after UV irradiation was dependent on Rad3 but not on Chk1 or Cds1. Taken together, these results suggest a function of Rad3 in the regulation of DNA damage repair that is distinct from those of other checkpoint proteins.

An alternative explanation of the ability of multicopy Cut8 (and separase/Cut1) to rescue *rad3* *rqh1* synthetic lethality is that precocious cleavage of cohesin reduces spontaneous recombination events between sister chromatids, thereby suppressing the hyper-recombination effect of the *rqh1* mutants. However, the *cut8* defect in DSB repair is unlikely to be an indirect negative effect on HR, as sister chromatids remain closely associated during interphase and this persists even after cells enter mitosis in the absence of Cut8 (27). A more direct role is suggested by the DNA repair function of securin-separase acting through the cleavage of cohesin (21), which could be needed following the enrichment of cohesin at DSB sites (24, 28). Cut8 might function with the securin-separase complex to aid DNA repair by removing local cohesin in interphase, thereby suppressing the synthetic lethality between *rad3* and *rqh1*. Alternatively, proteasome function mediated by Cut8 could be required for efficient DSB repair. It will therefore be of considerable interest to determine whether particular repair proteins are subjected to degradation by the proteasome. Further experiments are required to explore these possibilities and determine the requirement of Rad3 in these activities.

In summary, our data are consistent with a function of Rad3 and Cut8 in the modification of chromatin structure that is required for efficient DNA repair. Together with Rqh1-Top3, these functions are presumably required to process or disrupt aberrant recombination structures that arise during S phase to allow proper chromosome segregation during mitosis. Homologues of Cut8 have been identified in *Metazoa* (26); thus, it is likely that inhibition of Cut8 activity could generally be detrimental to genome stability.

ACKNOWLEDGMENTS

We thank A. M. Carr, P. Russell, M. Yamamoto, and M. Yanagida for yeast strains, H. Yamano for Cdc2 antibody, and E. C. Chang for plasmids.

This work was supported by Cancer Research UK and the Wellcome Trust Research Career Development Fellowship to S.-W. Wang.

REFERENCES

- Bachrati, C. Z., and I. D. Hickson. 2003. RecQ helicases: suppressors of tumorigenesis and premature aging. *Biochem. J.* **374**:577–606.
- Barbet, N., W. J. Muriel, and A. M. Carr. 1992. Versatile shuttle vectors and genomic libraries for use with *Schizosaccharomyces pombe*. *Gene* **114**:59–66.
- Bennett, R. J., and J. C. Wang. 2001. Association of yeast DNA topoisomerase III and Sgs1 DNA helicase: studies of fusion proteins. *Proc. Natl. Acad. Sci. USA* **98**:11108–11113.
- Carr, A. M. 2002. DNA structure dependent checkpoints as regulators of DNA repair. *DNA Repair (Amsterdam)* **1**:983–994.
- Coulon, S., P. H. Gaillard, C. Chahwan, W. H. McDonald, J. R. Yates III, and P. Russell. 2004. Slx1-Slx4 are subunits of a structure-specific endonuclease that maintains ribosomal DNA in fission yeast. *Mol. Biol. Cell* **15**:71–80.
- Du, L. L., T. M. Nakamura, B. A. Moser, and P. Russell. 2003. Retention but not recruitment of Crb2 at double-strand breaks requires Rad1 and Rad3 complexes. *Mol. Cell. Biol.* **23**:6150–6158.
- Ferreira, M. G., and J. P. Cooper. 2004. Two modes of DNA double-strand break repair are reciprocally regulated through the fission yeast cell cycle. *Genes Dev.* **18**:2249–2254.
- Foray, N., A. Priestley, G. Alsheih, C. Badie, E. P. Capulas, C. F. Arlett, and E. P. Malaise. 1997. Hypersensitivity of ataxia telangiectasia fibroblasts to ionizing radiation is associated with a repair deficiency of DNA double-strand breaks. *Int. J. Radiat. Biol.* **72**:271–283.
- Funakoshi, M., X. Li, I. Velichutina, M. Hochstrasser, and H. Kobayashi. 2004. Sem1, the yeast ortholog of a human BRCA2-binding protein, is a component of the proteasome regulatory particle that enhances proteasome stability. *J. Cell Sci.* **117**:6447–6454.
- Grishchuk, A. L., R. Kraehenbuehl, M. Molnar, O. Fleck, and J. Kohli. 2004. Genetic and cytological characterization of the RecA-homologous proteins Rad51 and Dmc1 of *Schizosaccharomyces pombe*. *Curr. Genet.* **44**:317–328.
- Hirano, T. 2005. Cell biology: holding sisters for repair. *Nature* **433**:467–468.
- Jeggio, P. A., A. M. Carr, and A. R. Lehmann. 1998. Splitting the ATM: distinct repair and checkpoint defects in ataxia-telangiectasia. *Trends Genet.* **14**:312–316.
- Krogan, N. J., M. H. Lam, J. Fillingham, M. C. Keogh, M. Gebbia, J. Li, N. Datta, G. Cagney, S. Buratowski, A. Emili, and J. F. Greenblatt. 2004. Proteasome involvement in the repair of DNA double-strand breaks. *Mol. Cell* **16**:1027–1034.
- Laursen, L. V., E. Ampatzidou, A. H. Andersen, and J. M. Murray. 2003. Role for the fission yeast RecQ helicase in DNA repair in G₂. *Mol. Cell. Biol.* **23**:3692–3705.
- Lopes, M., C. Cotta-Ramusino, A. Pelliccioli, G. Liberi, P. Plevani, M. Muzi-Falconi, C. S. Newlon, and M. Foiani. 2001. The DNA replication checkpoint response stabilizes stalled replication forks. *Nature* **412**:557–561.
- Martinho, R. G., H. D. Lindsay, G. Flagg, A. J. DeMaggio, M. F. Hoekstra, A. M. Carr, and N. J. Bentley. 1998. Analysis of Rad3 and Chk1 protein kinases defines different checkpoint responses. *EMBO J.* **17**:7239–7249.
- Mochida, S., and M. Yanagida. 2006. Distinct modes of DNA damage response in *S. pombe* G0 and vegetative cells. *Genes Cells* **11**:13–27.
- Moreno, S., A. Klar, and P. Nurse. 1991. Molecular genetic analysis of fission yeast *Schizosaccharomyces pombe*. *Methods Enzymol.* **194**:795–823.
- Murakami, H., and H. Okayama. 1995. A kinase from fission yeast responsible for blocking mitosis in S phase. *Nature* **374**:817–819.
- Murray, J. M., H. D. Lindsay, C. A. Munday, and A. M. Carr. 1997. Role of *Schizosaccharomyces pombe* RecQ homolog, recombination, and checkpoint genes in UV damage tolerance. *Mol. Cell. Biol.* **17**:6868–6875.
- Nagao, K., Y. Adachi, and M. Yanagida. 2004. Separase-mediated cleavage of cohesin at interphase is required for DNA repair. *Nature* **430**:1044–1048.
- Pâques, F., and J. E. Haber. 1999. Multiple pathways of recombination induced by double-strand breaks in *Saccharomyces cerevisiae*. *Microbiol. Mol. Biol. Rev.* **63**:349–404.
- Shimada, T., A. Yamashita, and M. Yamamoto. 2003. The fission yeast meiotic regulator Mei2p forms a dot structure in the horse-tail nucleus in association with the *sme2* locus on chromosome II. *Mol. Biol. Cell* **14**:2461–2469.
- Ström, L., H. B. Lindroos, K. Shirahige, and C. Sjogren. 2004. Postreplicative recruitment of cohesin to double-strand breaks is required for DNA repair. *Mol. Cell* **16**:1003–1015.
- Symington, L. S. 2002. Role of *RAD52* epistasis group genes in homologous recombination and double-strand break repair. *Microbiol. Mol. Biol. Rev.* **66**:630–670.
- Takeda, K., and M. Yanagida. 2005. Regulation of nuclear proteasome by Rhp6/Ubc2 through ubiquitination and destruction of the sensor and anchor Cut8. *Cell* **122**:393–405.
- Tatebe, H., and M. Yanagida. 2000. Cut8, essential for anaphase, controls localization of 26S proteasome, facilitating destruction of cyclin and Cut2. *Curr. Biol.* **10**:1329–1338.
- Unal, E., A. Arbel-Eden, U. Sattler, R. Shroff, M. Lichten, J. E. Haber, and D. Koshland. 2004. DNA damage response pathway uses histone modifica-

- tion to assemble a double-strand break-specific cohesin domain. *Mol. Cell* **16**:991–1002.
29. **Walworth, N., S. Davey, and D. Beach.** 1993. Fission yeast *chk1* protein kinase links the *rad* checkpoint pathway to *cdc2*. *Nature* **363**:368–371.
 30. **Wang, S. W., C. Norbury, A. L. Harris, and T. Toda.** 1999. Caffeine can override the S-M checkpoint in fission yeast. *J. Cell Sci.* **112**:927–937.
 31. **Win, T. Z., A. Goodwin, I. D. Hickson, C. J. Norbury, and S. W. Wang.** 2004. Requirement for *Schizosaccharomyces pombe* Top3 in the maintenance of chromosome integrity. *J. Cell Sci.* **117**:4769–4778.
 32. **Win, T. Z., H. W. Mankouri, I. D. Hickson, and S. W. Wang.** 2005. A role for the fission yeast *Rqh1* helicase in chromosome segregation. *J. Cell Sci.* **118**:5777–5784.
 33. **Wu, L., S. L. Davies, P. S. North, H. Goulaouic, J. F. Riou, H. Turley, K. C. Gatter, and I. D. Hickson.** 2000. The Bloom's syndrome gene product interacts with topoisomerase III. *J. Biol. Chem.* **275**:9636–9644.
 34. **Wu, L., and I. D. Hickson.** 2003. The Bloom's syndrome helicase suppresses crossing over during homologous recombination. *Nature* **426**:870–874.
 35. **Yen, H. C., C. Gordon, and E. C. Chang.** 2003. *Schizosaccharomyces pombe* *Int6* and Ras homologs regulate cell division and mitotic fidelity via the proteasome. *Cell* **112**:207–217.